

Optimization of Proportional Integral Controller's Gain for Speed Control in Direct Torque Control Strategy Using Genetic Algorithm

Dr. Nour Mohammed^a, Dr. Benali Abdelkrim^a, Dr. Tadjeddine Ali^a, Dr. Bendelhoum Mohammed Sofiane^a

^aDepartment of Technologies, Nour Bachir University Center of El-Bayadh, Algeria

^aEmail: m.nour@cu-elbayadh.dz

Abstract: The use of PI controllers in electrical machine drives is often characterized by the high effect of motor parameters changing; the main purpose of the presented paper is to adapt both proportional and integral gains in order to perform and improve a closed-loop speed-controlled induction motor using direct torque control. First, a mathematical model is built using electrical and mechanical equations, then the DTC control method for the induction machine is presented based on relationship blocs; all those blocs are sensitized by the Simulink toolbox environment in MATLAB Software. The speed control is optimized by an optimized PI controller using genetic algorithm; the comparative simulation results are presented in order to claim the improvement of the system.

Keywords: PI controller, DTC direct torque control, IM induction motor, GA genetic algorithm.

1. Introduction

In recent years, the socioeconomic way of life has been increasingly inextricably linked to the efficient production and utilization of electrical energy. Synchronous generators generate electricity, but for the flexible and distributed power systems of the future, the induction machine as a variable speed generator or electric motor has become the ideal electrical drive.

In addition, the induction motor dominates a large part of the industry due to its robustness, low cost, and good performance. It can be powered directly from a power grid. Developments in power electronics and digital control have triggered the widespread use of induction motors for variable speed drives in most electrical drive applications **Bose B K (2002)**.

As a result, the development of control laws and the implementation of control strategies for this type of machine become a more interesting line of research. **Takahashi. I and T. Noguchi (1986)**, Direct Torque Control (DTC) is applied to AC drive systems to achieve high-performance torque control, the implementation of this control for induction motors was introduced in the 1980s by Depenbrock, Takahashi, and Noguchi as an alternative solution to Field Oriented Control FOC **Depenbrock. M (1988), Blaschke. F (1972)** with the aim of simplifying control algorithms and achieving similar or even better performance. The DTC control is commonly used with a voltage inverter (Voltage Source Inverter VSI) **Faraji, Vahid, and Davood Arab Khaburi. (2011)**.

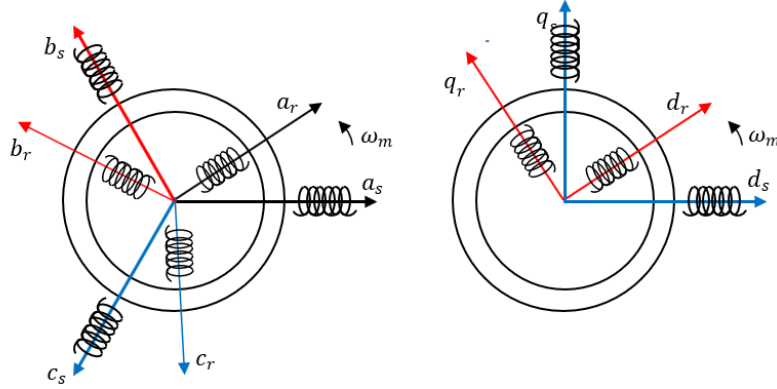
In our contribution, the problems caused by variations in machine parameters will be solved by the use of an adapted gain PI controller in the speed control loop. The performance thus obtained will be compared to that of the conventional PI controller.

2. Induction machine modeling

The model of the machine in the three-phase system is very complex, we appeal for its simplification in the transformation of Park. Physically, it can be explained by transforming three windings of the machine into just two windings as shown in figure 1 **Bose B K (2002)**.

In the Park transformation, the stator windings a_s, b_s, c_s and the rotor windings a_r, b_r, c_r are respectively transformed into two stator windings d_s, q_s and two rotor windings d_r, q_r . "d" refers to the direct axis and "q" to the quadrature axis. **Garces. L (1980)**.

$$[P(\theta_s)] = C \cdot \begin{bmatrix} \cos \theta_s & \cos(\theta_s - 2\pi/3) & \cos(\theta_s - 4\pi/3) \\ -\sin \theta_s & -\sin(\theta_s - 2\pi/3) & -\sin(\theta_s - 4\pi/3) \\ 1/\sqrt{2} & 1/\sqrt{2} & 1/\sqrt{2} \end{bmatrix} \quad (1)$$

Figure.1 Physical diagram of the *Park* transform


The previous transformations can also be applied to other quantities such as current or flux, so the values of the stator quantities is defined by:

$$\begin{bmatrix} i_{ds} \\ i_{qs} \\ i_{os} \end{bmatrix} = [P(\theta_s)] \begin{bmatrix} i_{as} \\ i_{bs} \\ i_{cs} \end{bmatrix}; \quad \begin{bmatrix} \phi_{ds} \\ \phi_{qs} \\ \phi_{os} \end{bmatrix} = [P(\theta_s)] \begin{bmatrix} \phi_{as} \\ \phi_{bs} \\ \phi_{cs} \end{bmatrix} \quad (2)$$

2.1 Electrical and magnetic equations in the Park coordinate system

The state representation in the stator-linked frame is used in the design of the direct torque control. This reference frame is denoted (α , β), it translates into the conditions $\frac{d\theta_s}{dt} = 0$ and $\frac{d\theta_r}{dt} = \omega_r$. The we obtain the following electrical equations **Bose B K (2002)**:

$$\begin{cases} v_{\alpha s} = R_s i_{\alpha s} + \frac{d\phi_{\alpha s}}{dt} \\ v_{\beta s} = R_s i_{\beta s} + \frac{d\phi_{\beta s}}{dt} \\ 0 = R_r i_{\alpha r} + \frac{d\phi_{\alpha r}}{dt} - \omega_m \phi_{\beta r} \\ 0 = R_r i_{\beta r} + \frac{d\phi_{\beta r}}{dt} + \omega_m \phi_{\alpha r} \end{cases} \quad (3)$$

By replacing the expressions of the currents of equation, we can write the equation of state of the induction machine in a coordinate system linked to the stator:

$$\frac{dX}{dt} = AX + BU \quad (4)$$

With:

$$X = \begin{bmatrix} \phi_{\alpha s} \\ \phi_{\beta s} \\ \phi_{\alpha r} \\ \phi_{\beta r} \end{bmatrix}; A = \begin{bmatrix} -\frac{R_s}{\sigma L_s} & 0 & \frac{MR_s}{\sigma L_s L_r} & 0 \\ 0 & -\frac{R_s}{\sigma L_s} & 0 & \frac{MR_s}{\sigma L_s L_r} \\ \frac{MR_r}{\sigma L_s L_r} & 0 & -\frac{R_r}{\sigma L_r} & -\omega_m \\ 0 & \frac{MR_r}{\sigma L_s L_r} & \omega_m & -\frac{R_r}{\sigma L_r} \end{bmatrix}; B = \begin{bmatrix} 1 & 0 \\ 0 & 1 \\ 0 & 0 \\ 0 & 0 \end{bmatrix} \quad \text{et } U = \begin{bmatrix} v_{\alpha s} \\ v_{\beta s} \end{bmatrix} \quad (5)$$

2.2 Expression of electromagnetic torque and mechanical speed

In a reference frame linked to the stator, the electromagnetic torque is expressed as a function of rotor and stator fluxes:

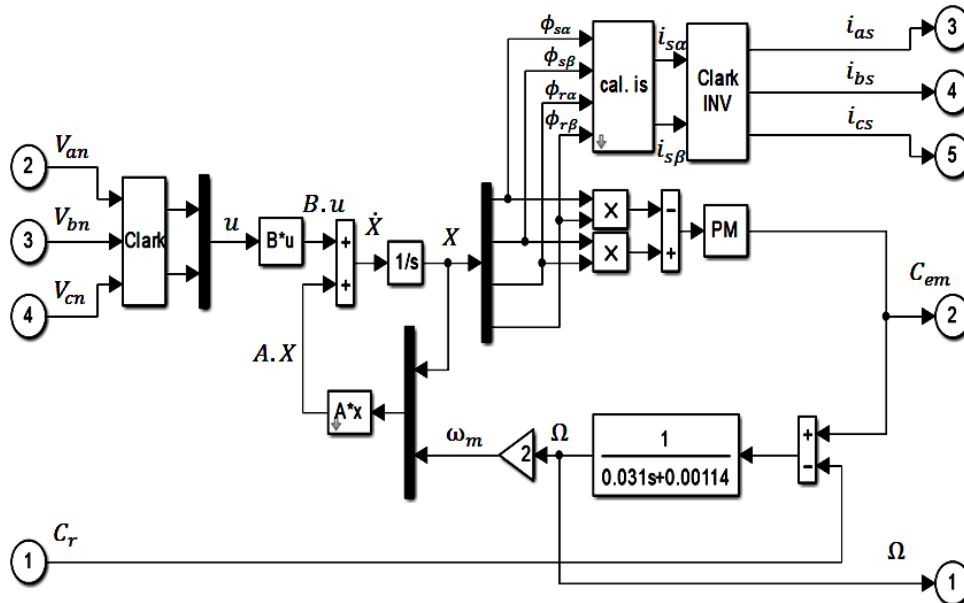
$$C_e = \frac{2}{3} P \frac{M}{\sigma L_s L_r} (\Phi_{ar} \Phi_{\beta s} - \Phi_{as} \Phi_{\beta r}) \quad (6)$$

The fundamental relationship of dynamics makes it possible to write:

$$C_e - C_r = J(d\Omega/dt) + f\Omega \quad (7)$$

Where C_e represents the electromagnetic torque produced by the motor, C_r the resistant torque, J the moment of inertia of all the rotating parts and f the coefficient of friction. This relationship is a differential equation whose variable is the angular velocity of the rotor. The relationships described above by the different equations can be represented by a diagram block using the *Simulink* environment (*MATLAB*) to perform a numerical simulation study and validate the dynamic model of the machine studied Wilamowski. B.M. & J.D. Irwin. (2018).

Figure.2 Simulink model of the induction machine



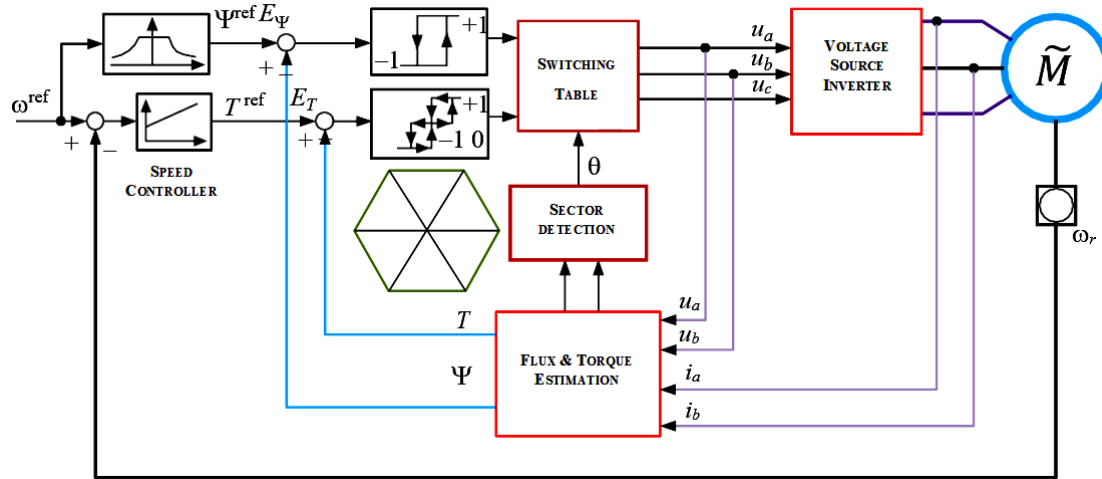
3. Direct torque control presentation

The direct torque control of an induction machine is based on the direct determination of the control sequence applied to the switches on a voltage source inverter.

This choice is generally based on the use of hysteresis comparators whose function is to control the state of the system, namely here the amplitude of the stator flux and the electromagnetic torque. Figure 3 demonstrates that the estimated value of the stator flux is compared to its desired value and the estimated value of the electromagnetic torque is compared to the torque generated by the speed controller.

The resulting flux and torque errors are used by two hysteresis comparators Quang. N.P and J.A. Dittrich (2015), the corresponding output values, as well as the stator position (sector number 1 to 6), are used to select the appropriate voltage vector from a selection table designed to generate the pulses for controlling the inverter switches T. Terras, K. Hatani (2020).

Figure.3 General structure of direct torque control



3.1 Estimation of stator flux and electromagnetic torque

Estimation of the flux sector position and amplitude

From the model of the induction machine in a stator-frame coordinate system and the expression of the stator voltage, the stator flux is estimated from the following relationship **Nour M, Tedjini H, Gasbaoui B (2019)**:

$$\phi_s = \int (v_s - R_s i_s) dt \quad (8)$$

The amplitude of the stator flux is estimated from its two-phase components $\phi_{s\alpha}$ and $\phi_{s\beta}$:

$$\phi_s = \sqrt{\phi_{s\alpha}^2 + \phi_{s\beta}^2} \quad (9)$$

Where $\phi_{s\alpha}$ and $\phi_{s\beta}$ are estimated using equation 8 which requires knowledge of the components of the stator current vector $i_{s\alpha}$, $i_{s\beta}$ and the stator voltage vector $V_{s\alpha}$, $V_{s\beta}$. **S.Krim, S. Gdaim, A. Mtibaa, M. F. Mimouni (2017)**.

Tazerart, F, Z. Mokrani, D. Rekioua, and T. Rekioua (2015). The components of the stator current vector are obtained by applying the Concordia transformation to the measured three-phase components i_{sa} , i_{sb} and i_{sc} :

$$\begin{cases} i_{s\alpha} = \sqrt{\frac{3}{2}} i_{sa} \\ i_{s\beta} = \frac{1}{\sqrt{2}} (i_{sb} - i_{sc}) \end{cases} \quad (10)$$

The components of the stator voltage vector are obtained from the states of the switches **Nour M, Tedjini H, Gasbaoui B (2019)**:

$$\begin{cases} v_{s\alpha} = \sqrt{\frac{3}{2}} E \left[S_a - \frac{1}{2} (S_b + S_c) \right] \\ v_{s\beta} = r \cdot \sqrt{\frac{3}{2}} E (S_b - S_c) \end{cases} \quad (11)$$

Estimation of electromagnetic torque

The electromagnetic torque can be estimated from the flux estimation and the current measurement using the expression of the torque as a function of the flux and the stator current given by the equation:

$$C_e = P (\phi_{s\alpha} i_{s\beta} - \phi_{s\beta} i_{s\alpha}) \quad (12)$$

3.2 Developing the switching table

The table of the control structure is elaborated, according to the outputs of the flux hysteresis controller ($d\phi_s$), the torque hysteresis controller (dC_{em}), and the N zone of the stator flux vector position. We find with the control table, the selection of voltage vectors V_{i-1} , V_{i+1} , V_{i-2} , V_{i+2} correspond to a zone i ;

This section shall be carried out at each sampling period T_e using the switching tables proposed by *Takahashi*.

Table.1. Switches for a two-level hysteresis comparator

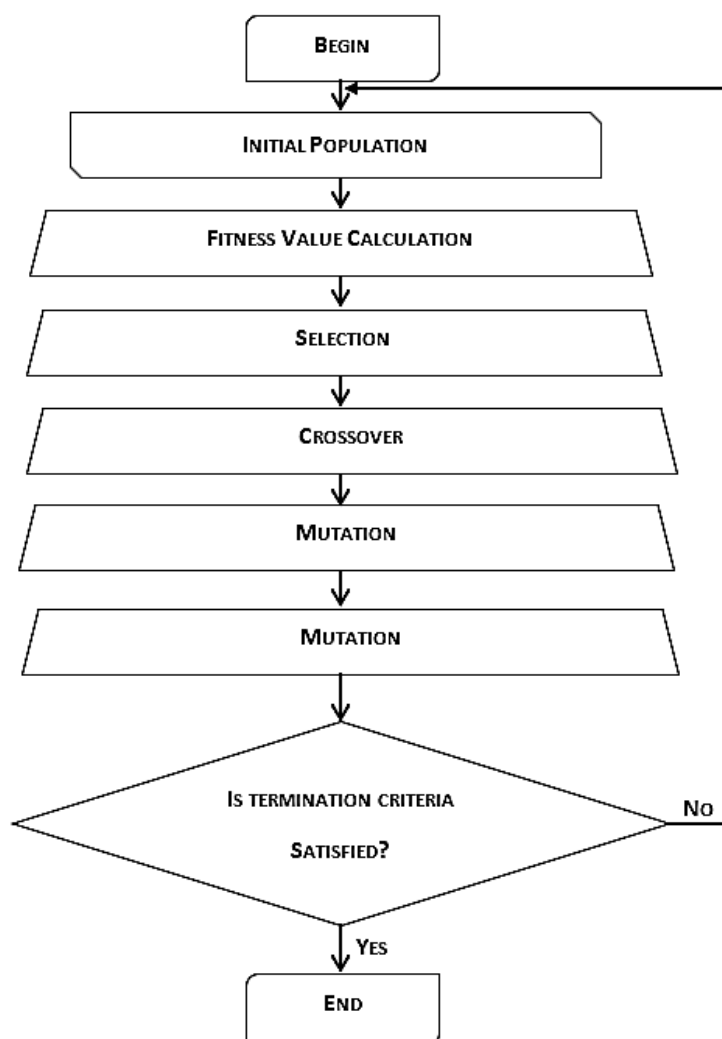
<i>N</i>		<i>1</i>	<i>2</i>	<i>3</i>	<i>4</i>	<i>5</i>	<i>6</i>
<i>dφ_s</i>	<i>dC_{em}</i>						
<i>1</i>	<i>1</i>	<i>V₂</i>	<i>V₃</i>	<i>V₄</i>	<i>V₅</i>	<i>V₆</i>	<i>V₁</i>
	<i>0</i>	<i>V₇</i>	<i>V₀</i>	<i>V₇</i>	<i>V₀</i>	<i>V₇</i>	<i>V₀</i>
<i>0</i>	<i>1</i>	<i>V₃</i>	<i>V₄</i>	<i>V₅</i>	<i>V₆</i>	<i>V₁</i>	<i>V₂</i>
	<i>0</i>	<i>V₀</i>	<i>V₇</i>	<i>V₀</i>	<i>V₇</i>	<i>V₀</i>	<i>V₇</i>

3.3 Speed control with genetic algorithm PI adaptation

The PI Proportional and Integral Action Corrector covers a wide range of industrial applications. It is used to generate the control torque from the deviation of the actual and reference quantities of the rotor speed of the induction machines controlled by the DTC. This use is characterized by overtaking in pursuit mode and a slow rejection of load disturbances. This is mainly caused by the fact that the gains of the PI controller cannot be adjusted to solve at the same time the problem of overtaking and of slow rejection of load disturbances. A setting for the elimination of overtaking will result in a very slow rejection of disturbances, and a setting for rapid rejection of disturbances will result in a significant exceedance **Y. Belgaid , M. Helaimi , R. Taleb , M BenaliYoucef (2020).**

In order to counter this problem, it is proposed to use variable gain PI controllers using GA.

Figure.4 The general structure of genetic algorithm



Optimization is the process of determining the optimal solution to a problem in terms of one or more predefined criteria while considering the system's characteristics and enforced limitations. Using random

processes, the ideal solution is selected from a population of solutions. The search for the optimal solution is predicated on the formation of new solutions by the sequential application of three operators to the current population: selection, crossing, and mutation. These processes are repeated until a criterion for stopping is met **Y. Belgaid , M. Helaimi , R. Taleb , M BenaliYoucef (2020)**. Figure 4 illustrates a straightforward Genetic Algorithm principle.

4. Simulation results

In order to study the performance of the previously synthesized regulator, a comparative simulation study was carried out, using the same Simulink model of the DTC control, with the replacement of the PI regulator -used in the speed loop- by a genetic algorithm adapted PI controller in the DTC control part.

Figure 5 shows the reaction of the two regulators to the variation in stator resistance. The motor is started under load and at time $t=2$ s the stator resistance is increased by 50% for two seconds. The PI regulator has a speed overrun of 1.14%, a speed drop of 1.14% and a rejection time of 0.9 s. The proposed controller maintains the speed at its reference value. It appears to be very robust to the variation of stator resistance.

The simulation shown in Figure 6 shows the dynamic performance of the two regulators during laden start-up with application of ± 5 N.m of load disturbance at 2 s and 4 s respectively. The machine is started with a load of 10 N.m and undergoes at $t = 2$ s a 50% increase in load for a period of 2 secs. For the PI regulator, the engine speed reaches Ω_{ref} with a response time of 0.193 s and an overshoot of 1.14%. The application of the disturbance causes the speed to drop by 6.2% compared to the set point, before returning to it after 1.4 s.

For the adapted regulator, the response time is reduced (0.126 s) and the exceedance is completely canceled. Application of the disturbance causes the speed to drop by 0.1% with a rejection time of 0.06 s.

For both controllers, the starting current takes a maximum value of 25.5 A, and then decreases rapidly to its nominal value. There is an increase of 1.56 A during the application of the disturbance.

The torque takes a maximum value of 38.3 N.m at the time of start-up, and then decreases rapidly to the nominal value. It follows the path of the disturbance with a response time of 0.10 s for the classical PI. While for the new controller, the response time to the disturbance tends towards zero. The torque has a ripple of 0.3 N.m for both cases.

Figure.5 Robustness test (variation of R_s (50%))

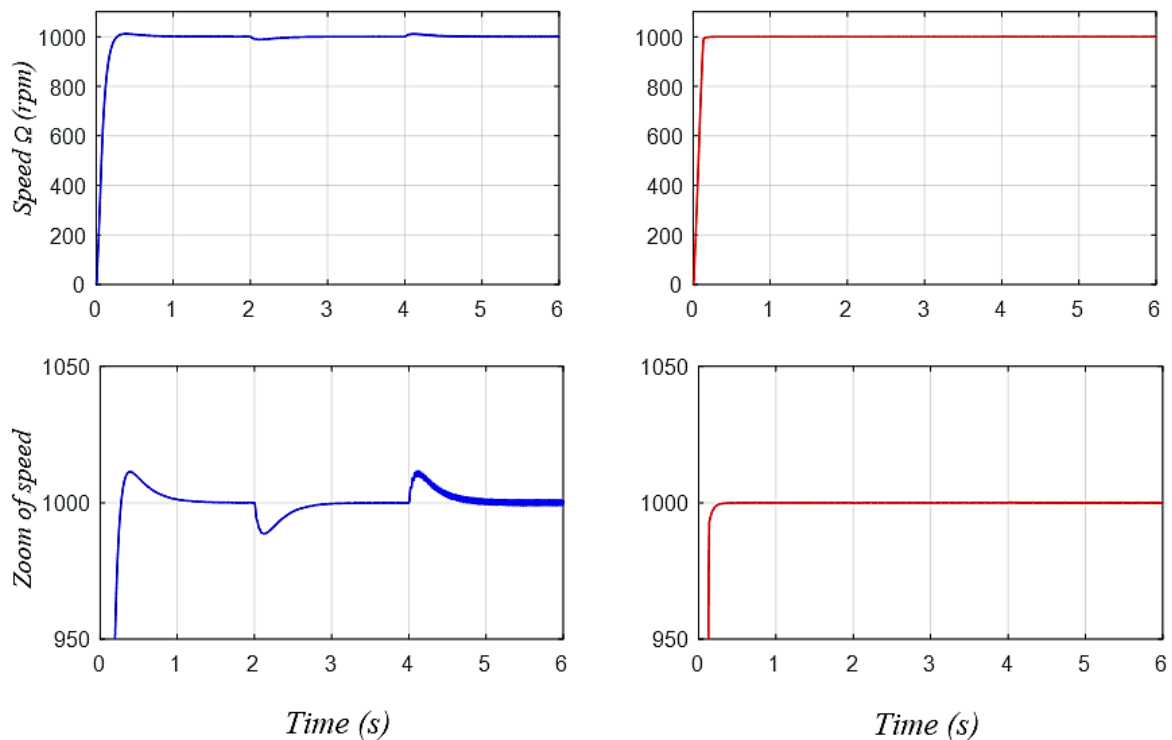
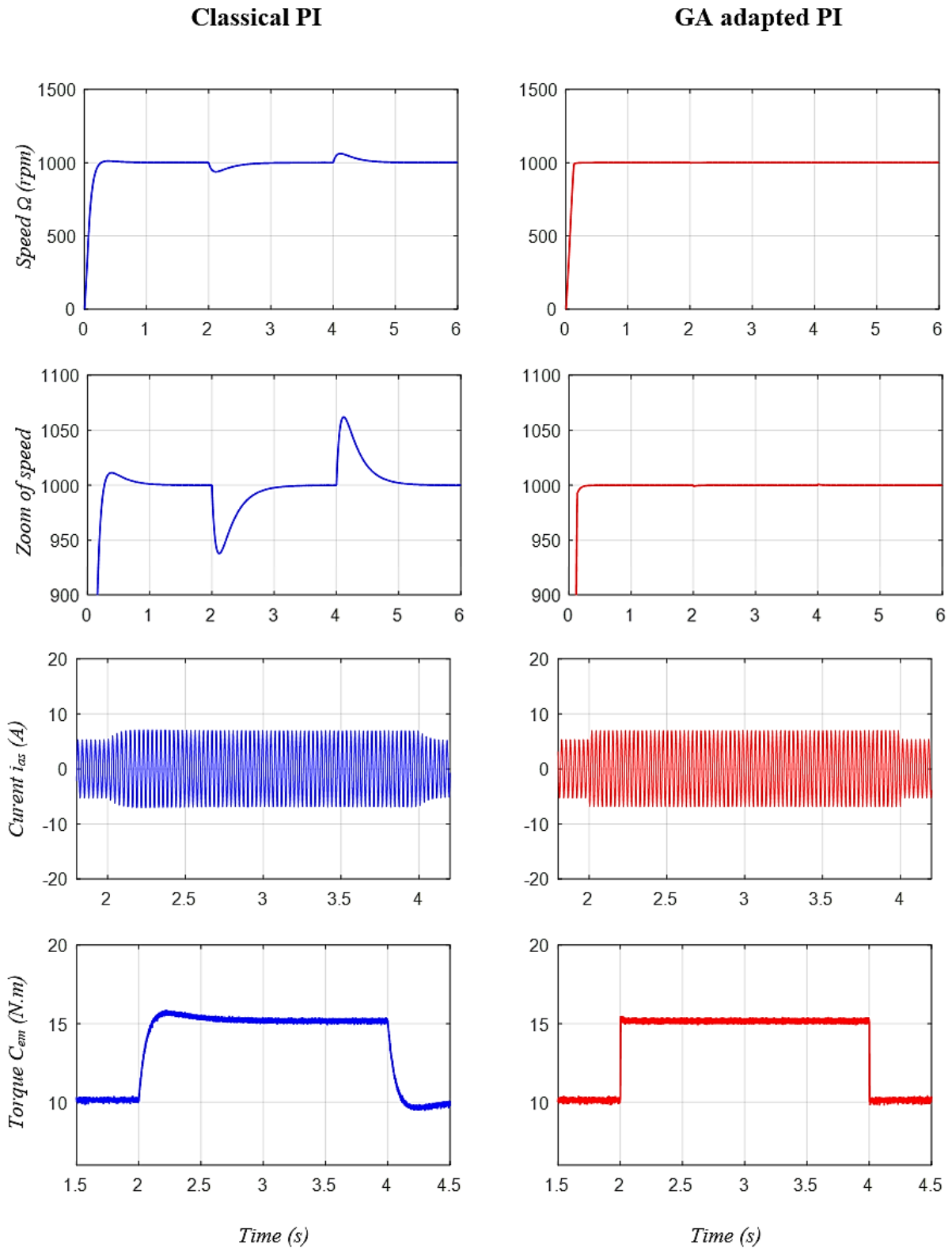


Figure.6 [The Performance Comparison When Booting up with \$\pm 5\$ N.m Load Disturbance Application](#)



5. Conclusion

The results of the simulations developed for the speed control optimized by a PI regulator based on genetic algorithms clearly illustrate that this controller remains more efficient than the conventional PI regulator. The proposed regulator showed the following performance:

- Total elimination of overrun and considerable reduction in start-up time.

- Significant reduction in the rejection time of load disturbances with a small speed drop.
- Good support for variations in engine parameters.

In conclusion, the usefulness of regulating the speed of an asynchronous motor by a DTC approach was justified by simulation. The summary of the results obtained clearly shows that this control is by far more efficient than conventional orders.

Finally, special efforts will have to be made to validate our study, at each stage, using an experimental study. Finally, our work carried out during this thesis would be more valid and concrete by the implementation in practice of our order and the validation of the results obtained via experimental tests.

References

- Bose B K (2002). *Modern Power Electronics and AC Drives*, Prentice Hall PTR.
- Takahashi. I and T. Noguchi (1986). A New Quick-Response and High-Efficiency Control Strategy of an Induction Motor, *IEEE Transactions on Industry Applications*, IA-22(5), p. 820-827.
- Depenbrock. M (1988). Direct self-control (DSC) of inverter-fed induction machine, *IEEE Transactions on Power Electronics*, 3(4), p. 420-429.
- Blaschke. F (1972). The principle of field oriented as applied to the new Tran vectorclosed loop control system for rotating machine, *Siemens review*, 39(5), p.217-220.
- Garces. L (1980) Parameter Adaption for the Speed-Controlled Static AC Drive witha Squirrel-Cage Induction Motor, Vol. IA-16, p. 173-178.
- Wilamowski. B.M. and J.D. Irwin. (2018). *Power Electronics and Motor Drives*, CRC Press.
- Y.Belgaid , M.Helaimi , R.Taleb , M BenaliYoucef (2020). Optimal tuning of PI controller using genetic algorithm for wind turbine application, *ijeecs*. v18.i1.pp167-178.
- T. Terras, K. Hatani (2020). Sensorless DTC of IPMSM for embedded systems, *ijpeds*. v11.i1.pp86-96
- Quang. N.P and J.A. Dittrich (2015). *Vector Control of Three-Phase AC Machines: System Development in the Practice*, Springer Berlin Heidelberg.
- Nour M, Tedjini H, Gasbaoui B (2019). Novel DTC induction machine drive improvement using controlled rectifier for DC voltage tuning, *ijpeds*.v10.i3.1223-1228
- Faraji, Vahid, and Davood Arab Khaburi. (2011). A new approach to DTC-ISVM for induction motor drive system fed by indirect matrix converter, 2nd Power Electronics Drive Systems and Technologies Conference.
- Tazerart. F, Z.Mokrani, D.Rekioua, and T.Rekioua (2015). Direct torque control implementation with losses minimization of induction motor for electric vehicle applications with high operating life of the battery, *International Journal of Hydrogen Energy*.
- S.Krim, S. Gdaim, A. Mtibaa, M. F.Mimouni (2017). FPGA-Based Implementation Direct Torque Control of Induction Motor, *(IJPEDS) Vol. 5, No. 3*, pp. 293~304.